



# **ATTACHMENT 1**

## **AIRWORTHINESS GROUP CHAIRMAN'S FACTUAL REPORT**

**CEN13FA192**

**Sikorsky Aircraft Corporation Tail Rotor Blade Materials Engineering  
Report No. MER-OA1308141 (16 Pages)**

**Note: Sikorsky authorized the placement of this proprietary document within the NTSB public docket for this investigation.**



**MATERIALS ENGINEERING REPORT**

SAMPLE IDENTIFICATION  Mishap A/C 760369 Tail Rotor Blade Examination	MODEL S-76A++	
	CHARGE NO. [REDACTED]	
	SUBMITTED BY NTSB	DATE 4/10/13

Background

The subject aircraft, registration N574EH, operated by Era Helicopters LLC, was destroyed upon impact near Grand Lake, Louisiana. The spar of the red/yellow blade had fractured at two locations and the 'red' and 'yellow' paddles were not recovered. The spar of the black/blue tail rotor blade fractured near the boot of the black paddle. An initial examination of the blades was performed by Sikorsky in April, 2013. The remnants of the red/yellow spar were examined in greater detail in August, 2013.

Examination

Figures 1 and 2 show the tail rotor blades as they were received by the laboratory in April of 2013. The blue/black blade paddles exhibited a relatively minor amount of damage, which indicates that they did not impact the ground with a significant degree rotational force. Fracture of the blue/black blade spar occurred just outboard of the boot on the black blade side. Fracture of the red/yellow blade spar occurred roughly at the pivot bearing location on the red blade side and at the edge of the retention plate assembly on the yellow side. The bonded pivot bearing retainers had separated from the pylon and outboard sides of the red blade spar half and were not recovered. The bumper plates, which are bonded to the spar at the same time as the retainer plates, remained with the spar.

Overall views showing the pylon and outboard sides of the spar fractures are given in Figures 3 and close-up views showing the center section of the red/yellow blade spar are given in Figure 4. The red/yellow blade was found to have shifted in the direction of the yellow blade. This is an indication that the red paddle departed the aircraft first with the resulting centrifugal force imbalance causing the spar to be pulled in yellow blade

[REDACTED]

Prepared by

[REDACTED]

[REDACTED]

Approved by

[REDACTED]

6/9/14

Date



direction. The force of the imbalance was sufficient to yield the aluminum center plug at the lightening holes, and force graphite splinters through the lightening hole wall. Once the blade had shifted within the retention plate, the yellow blade fractured at the edge of the retention plate assembly.

Close-up views of the blue/black blade spar fracture are given in Figure 5. Fracture occurred inboard of the pivot bearing at the bumper location. The fracture exhibited a broom straw appearance across the width with a flat compressive zone on the pylon side. The appearance was consistent with a flatwise bending overload fracture.

Close-up views of the red blade fracture are given in Figure 6. Fracture occurred outboard of the bumpers and exhibited a partial broom straw appearance with the longest broom straw strands in the center of the spar and becoming progressively shorter in the direction of the leading and trailing edge. The spar was noted to exhibit a chordwise bow and a mid-thickness delamination that extended across the width of the blade.

The yellow blade fracture is shown in Figure 7. The center portion of the spar had pulled away from the center plug and departed the aircraft with the rest of the blade. Only the leading and trailing ligaments remained. Fracture of the ligaments occurred at the edge of the retention plate. Unlike the black and red blade spar fractures, the yellow blade fracture showed no significant broom straw fracturing or inter-ply delaminations.

Following documentation of the as-received condition, the blades were removed from the retention plate and the blue/black blade spar was removed from the paddles. The spars were then x-ray inspected for evidence of ply waviness using the inspection procedure outlined in QATI 3210, Radiographic Inspection Procedure for P/N 7610-05016/76101-05017 Graphite Composite Tail Rotor Spar. No ply waviness or any other manufacturing anomaly was found; see Figure 8. This concluded the blade examination in April of 2013.

In August of 2013 the red/yellow spar was submitted for a more detailed examination. The spar piece was sectioned as shown in Figures 9 through 11. Close-up views of the yellow arm fracture are given in Figure 10. The fracture exhibited a predominately



tensile fracture appearance with a compressive fracture zone on the trailing side of the leading ligament.

The red arm fracture was opened at the mid-thickness delamination and examined for evidence of a progressive fracture; see Figures 12 and 13. One area of the delamination surface exhibited a powdery appearance that was thought to possibly be caused by rubbing, so the part was examined in greater detail in a scanning electron microscope; see Figures 14 through 16.

Examination of the delamination surface showed resin hackling, which is characteristic of shear fractures in graphite-epoxy laminates. The powdery appearance was due to the presence of numerous small particles of fractured resin that were found elsewhere on the fracture, but to a lesser degree. The fracture itself showed sharp features with no indication of the kind of rubbing damage that would be associated with a progressive fracture.

The pivot retainer separation surfaces exhibited a mixed mode of separation with adhesive disbond of the primer at the primer/metal interface and cohesive fracture of the rubber plus adhesive disbond of the primer at the rubber/primer interface; see Figures 17 through 19. The separation surface was examined in a scanning electron microscope in an attempt to determine the direction of separation; see Figures 20. Evidence for directionality was limited and inconsistent, so the direction of separation could not be determined.

#### Materials Examination

Samples of the spar were removed from the center section inboard of the yellow blade fracture and prepared for measurement of the fiber volume. The measured volume of fibers for three samples ranged from 59.1 to 60.5%; 55 to 65% was required.

The trailing edge of the spar was polished in the area between STA 0 and STA 3 as shown in Figures 9, and the number of plies was counted and compared to the drawing requirement; see Figure 21. The two +20° plies were located thirteen plies in from the surface on both the pylon and outboard sides of the spar, as required by the spar assembly drawing. A total of thirty-three plies were present. The drawing specifies thirty-three plies plus four optional plies. The thickness of the spar at that location measured .402 to .404"; .377 to .422" is required.

Conclusions

1. The paddles of the blue/black blade showed minimal damage, which indicates that they impacted the ground without a significant amount of rotational energy.
2. The blue/black blade spar had fractured at the pivot bumper location on the black blade side.
3. The black blade spar fracture exhibited a broom straw appearance and was accompanied by a thin strip of smooth, flat fracture on the pylon side. The overall appearance was consistent with a flatwise bending overload fracture.
4. The red paddle departed the aircraft before the yellow paddle. The resulting imbalance allowed the spar to shift in the yellow blade direction and deform the center plug.
5. Fracture of the red arm occurred at the pivot bearing location and exhibited a partial broom straw appearance with the strands longest in the center of the spar and becoming progressively shorter toward the edges.
6. The red blade spar remnant contained a mid-thickness delamination. The delamination was opened and examined for evidence of rubbing that would indicate a progressive fracture mode. No rubbing was found.
7. The yellow paddle departed the aircraft due to bending overload fracture at the edge of the blade retention plates.
8. The bonded pivot retainers on the red blade had separated from the spar and were not recovered. Examination of the bond surfaces showed a mixed mode of separation including adhesive disbond of the primer at the primer/rubber and primer/metal interfaces, plus cohesive fracture of the rubber. The direction of separation could not be definitively determined.

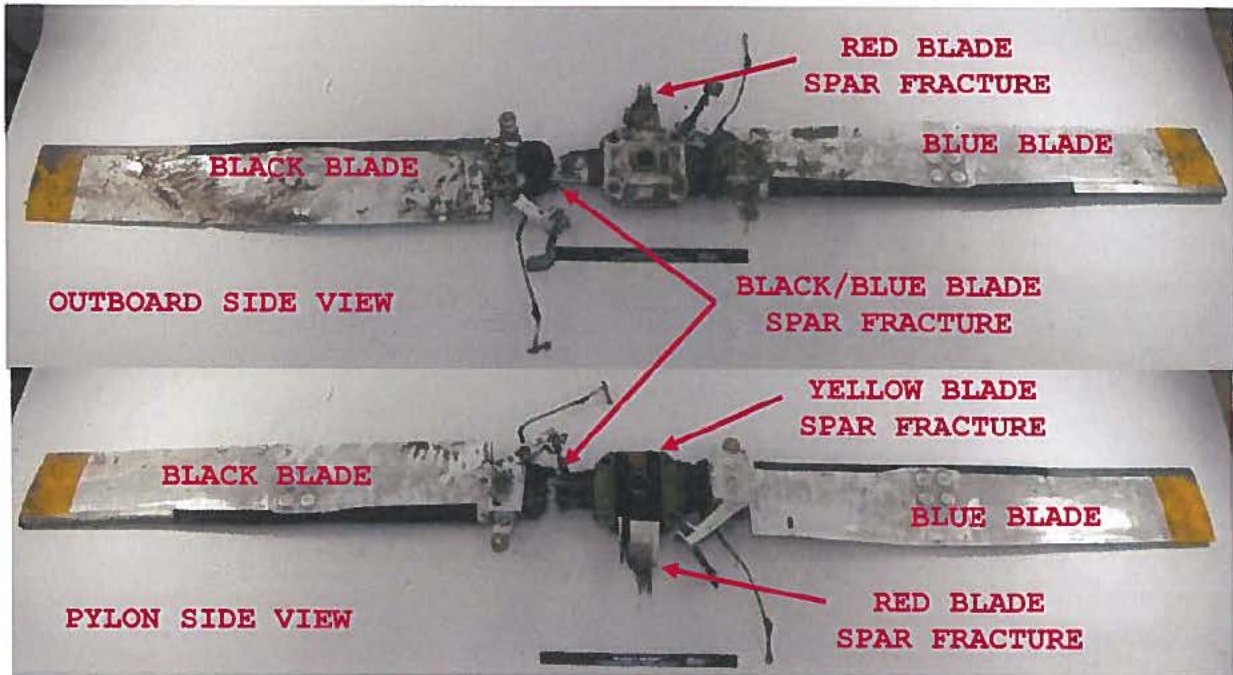


Figure 1

Overall photographs showing the as-received condition of the subject tail rotor blade pieces with associated hardware. Locations of the spar fractures are shown. Note paddles were in generally good condition.

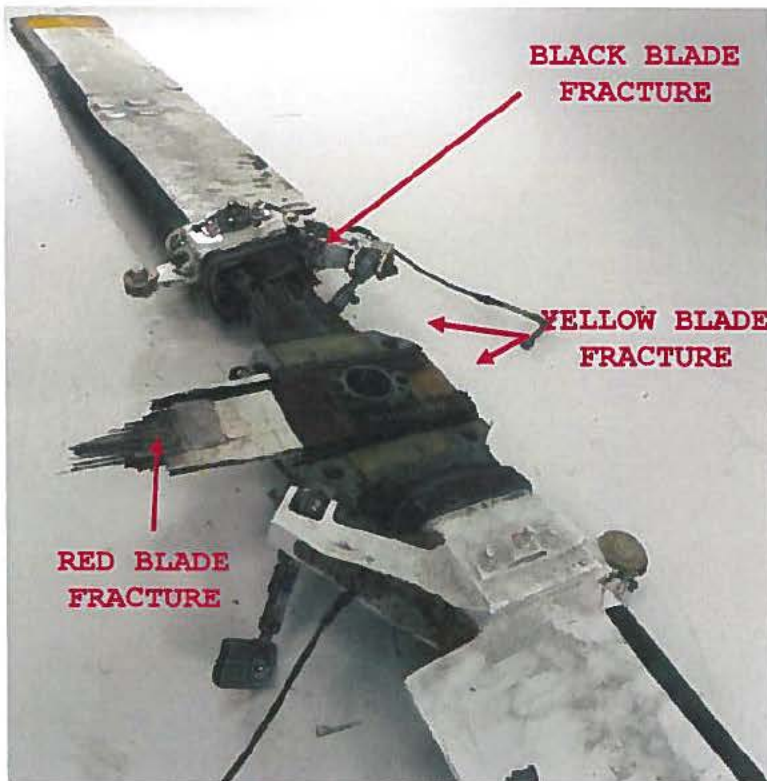


Figure 2

Close-up view of the pylon side showing the fracture locations.

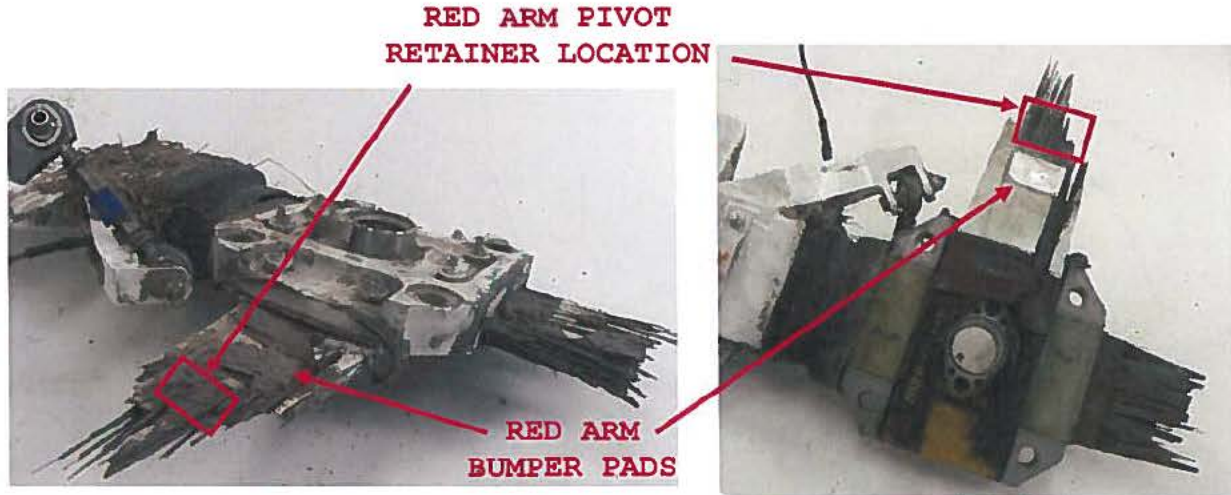


Figure 3

Another as-received view showing the outboard and pylon sides of the fractures.

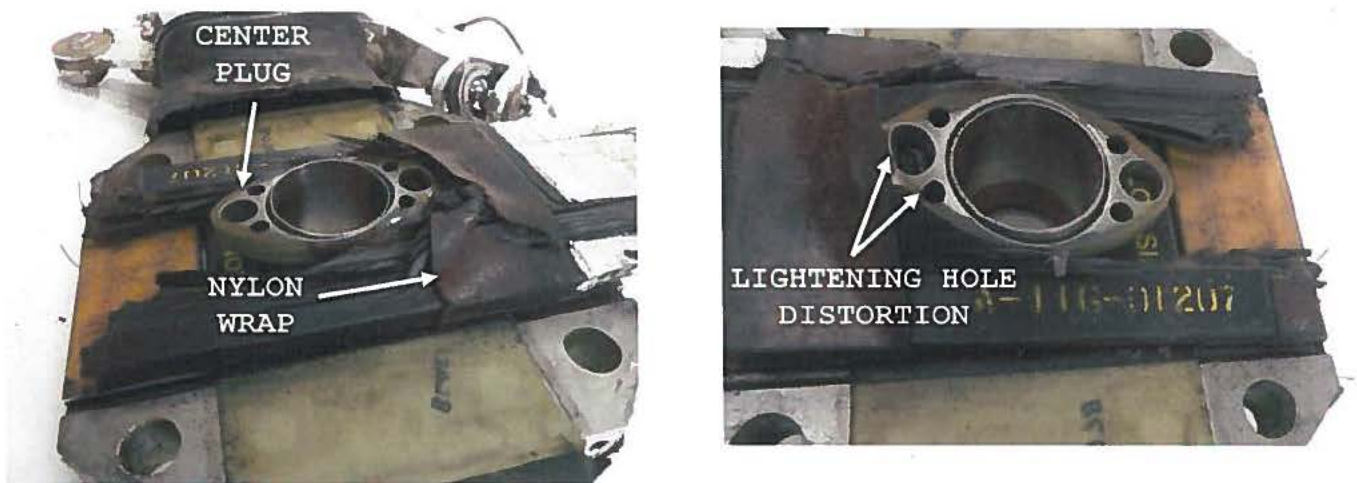
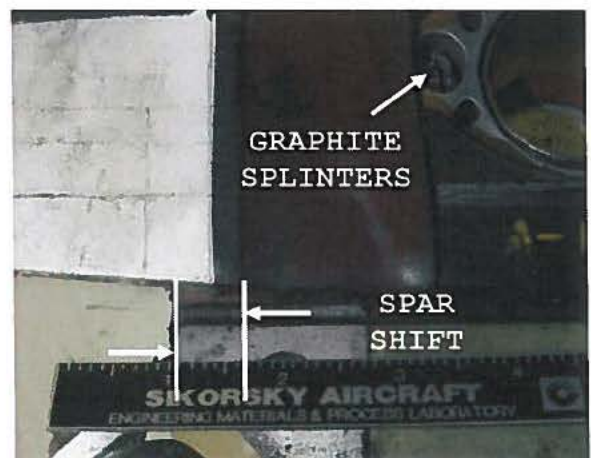


Figure 4

Close-up views of the red/yellow blade spar center section showing yielding of the center plug and graphite splinters that penetrated into the lightening hole. Spar shift is indicated by the location of the nylon wrap, which is aligned with the edge of the retention plate at installation.



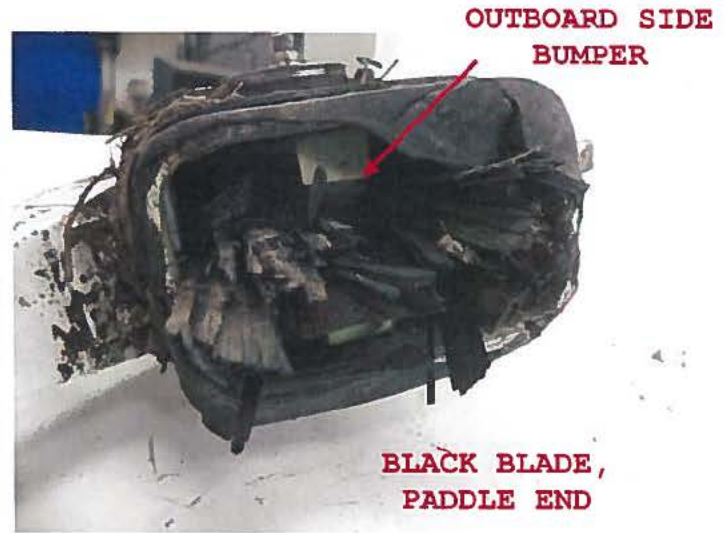


Figure 5

Views of the black arm spar fracture showing broom straw appearance of the fracture and compressive fracture area on the pylon side.

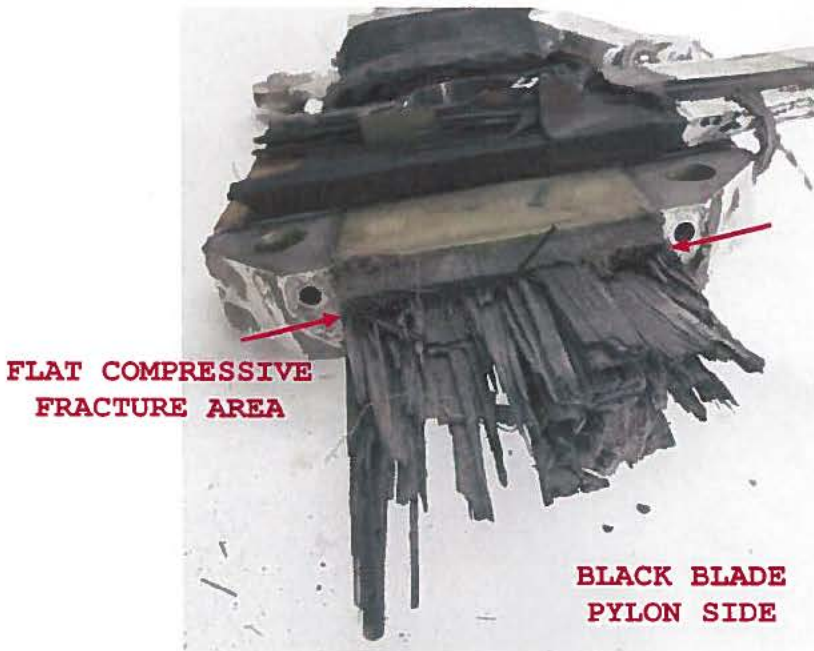


Figure 6 (below)

Views of the red arm blade spar fracture showing broom straw appearance of the center section and mid thickness delamination.

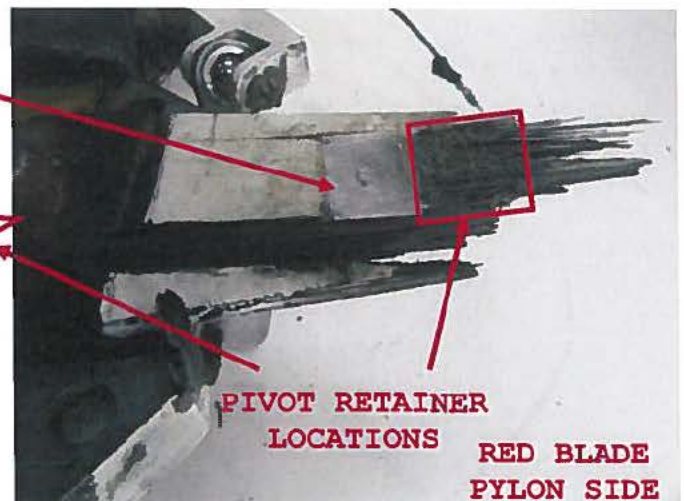
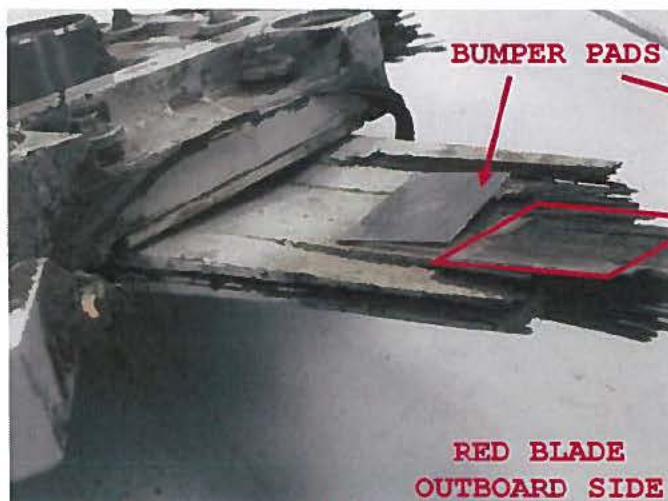




Figure 7

Close-up view of the yellow arm fracture. The leading and trailing ligaments of the fracture, still packed with mud in this view, exhibited a relatively flat fracture appearance with no obvious delamination or broom straw fractures.

**BLACK ARM**



**FLATWISE VIEW**



**EDGEWISE VIEW**

**BLUE ARM**



**FLATWISE VIEW**



**EDGEWISE VIEW**

**RED/YELLOW BLADE SPAR REMNANT**



Figure 8

Photos documenting the radiographic inspection results.



Figure 9

Outboard side of red/yellow blade spar remnants shown prior to sectioning. Dashed lines indicate saw cut locations. The center section was also used for fiber volume specimens.

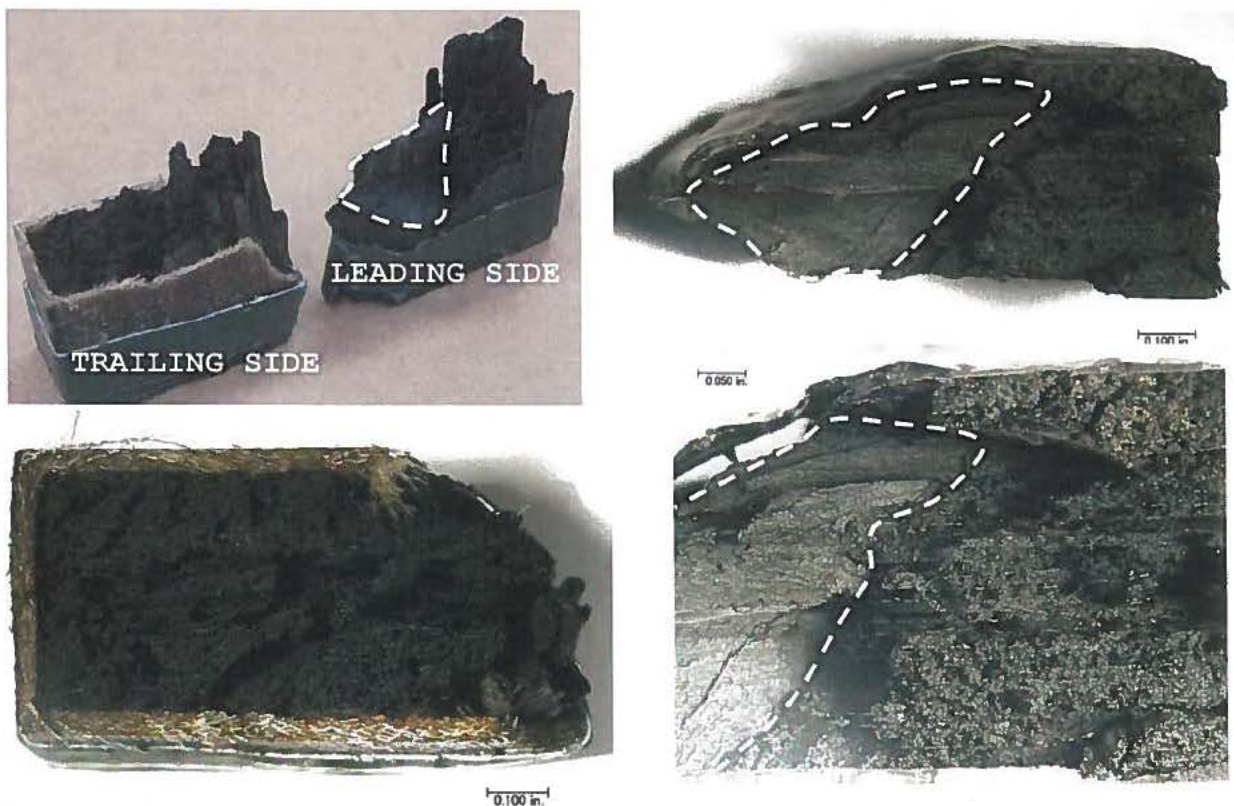


Figure 10

Overall and close-up views of the yellow blade fracture showing fractured fibers. Dashed line indicates the location of the rubbed region, correlating to the compressive portion of the fracture.



Figure 11

Close-up views of the red blade fracture after sectioning and prior to clam-shelling to expose the mid-thickness delamination surfaces. Pylon side shown.

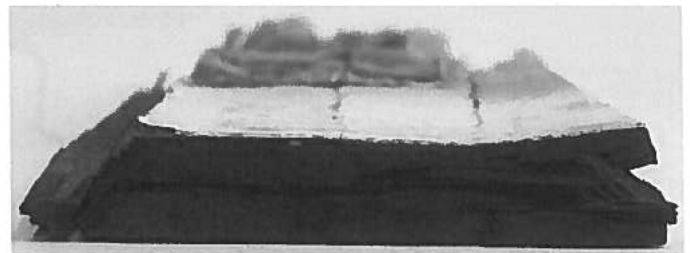


Figure 12

Red blade fracture surface shown after clam-shelling. Close-up views documenting the fracture appearance are given in Figures 13 through 16.



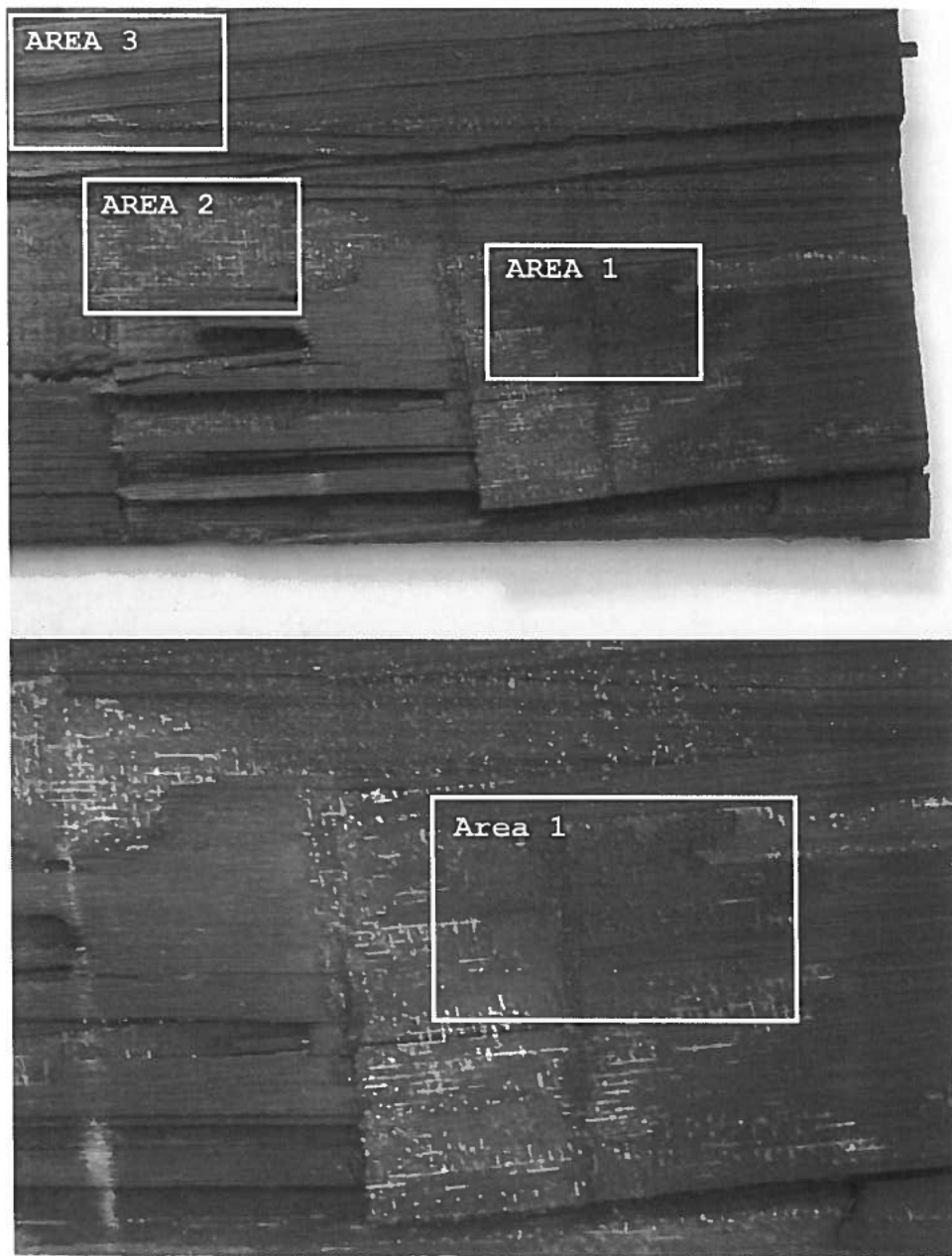


Figure 13

Close-up views of the delamination surface, which generally exhibited a fresh, static fracture appearance. The 'powdery' region, designated Area 1 was examined and compared to areas 2 and 3 in a scanning electron microscope. See Figures 14 through 16 for SEM views of these areas.

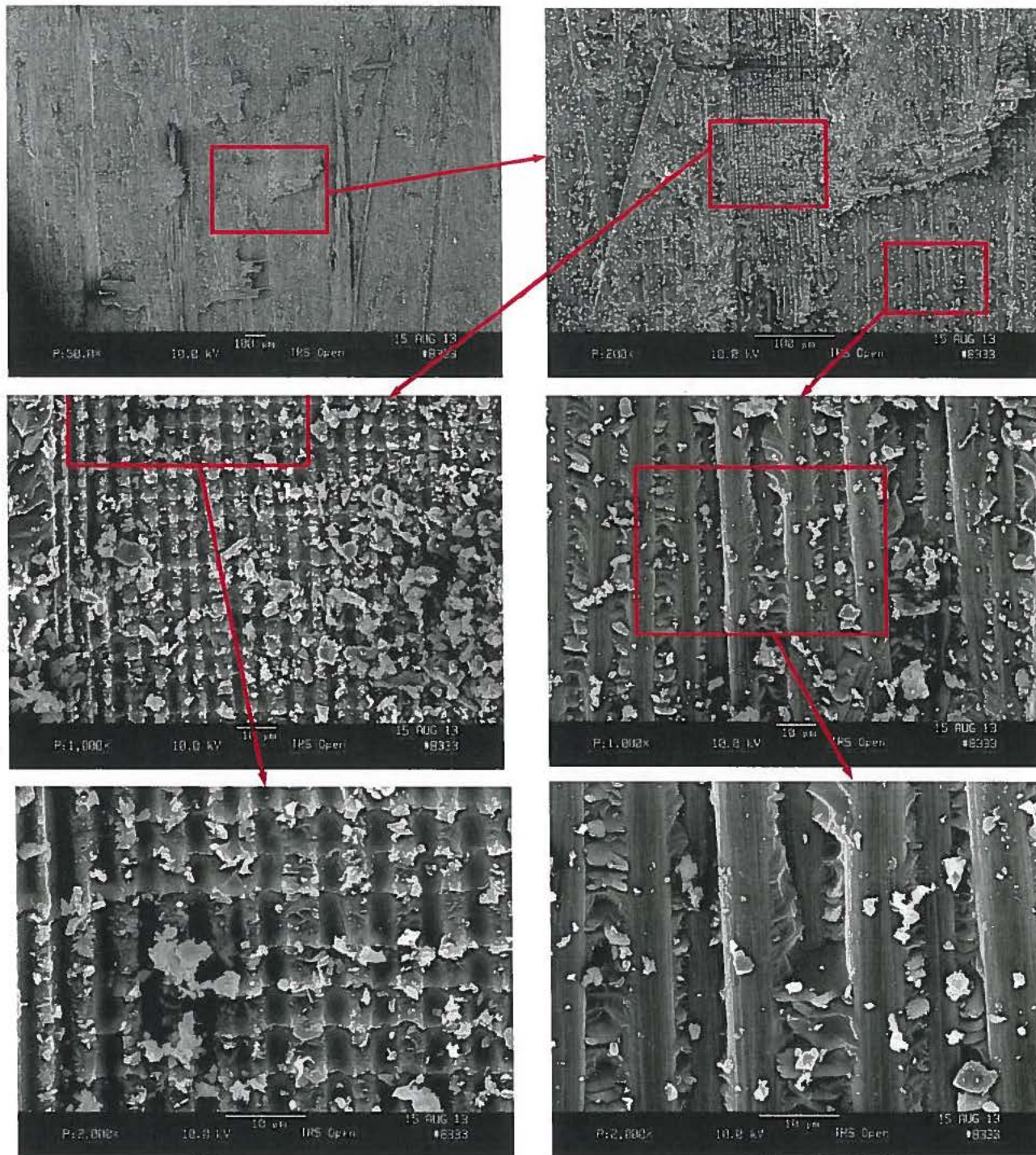


Figure 14

Successive magnification views of Area 1 showing the appearance of the delamination surface. Upper right view shows an impression from the fiberglass scrim (magnified views at left) and an area of graphite fibers (magnified views at right). Note thick build-up of loose resin particles on the fracture surface. At high magnification the resin fracture features are clearly defined. No rubbing is evident.

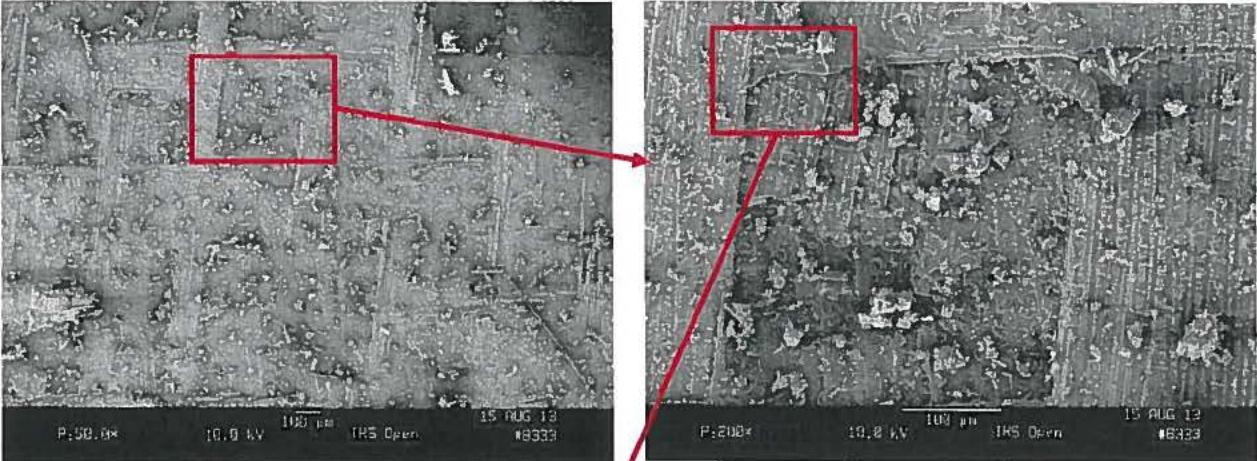


Figure 15

Successive magnification views of Area 2 showing many of the same features seen in Area 1.

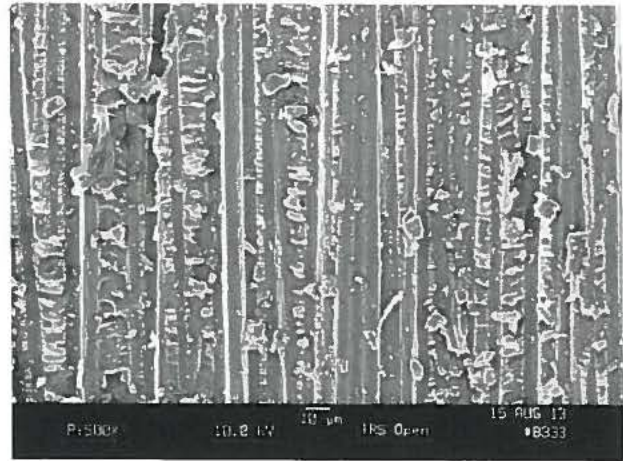
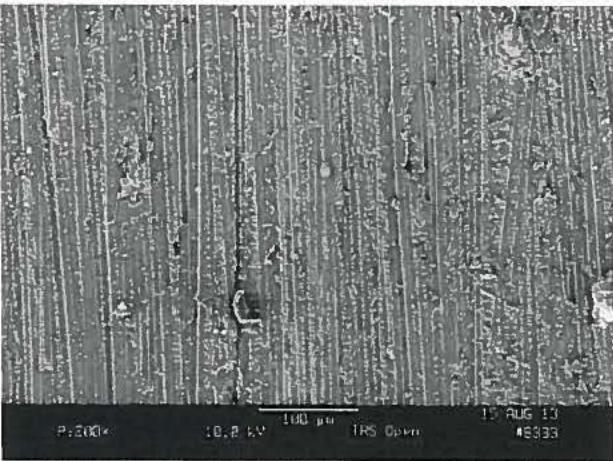
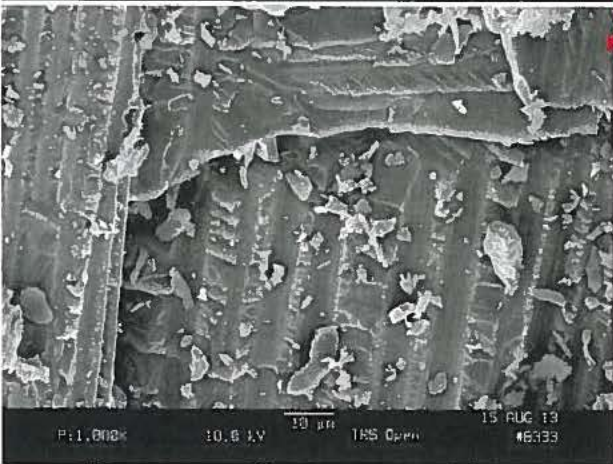
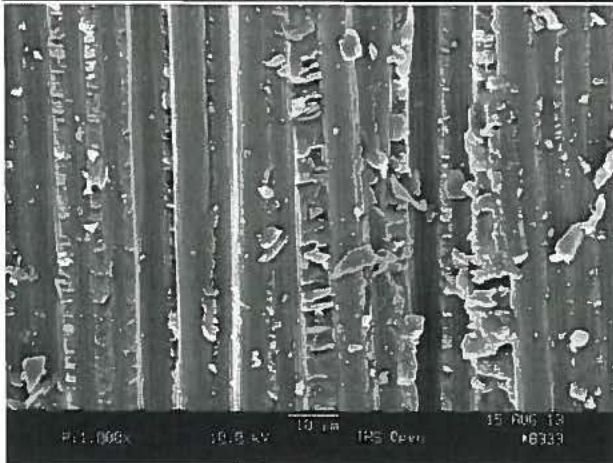


Figure 16

Successive magnification views of Area 3. Fewer particles of resin were visible on the delamination surface at this location.



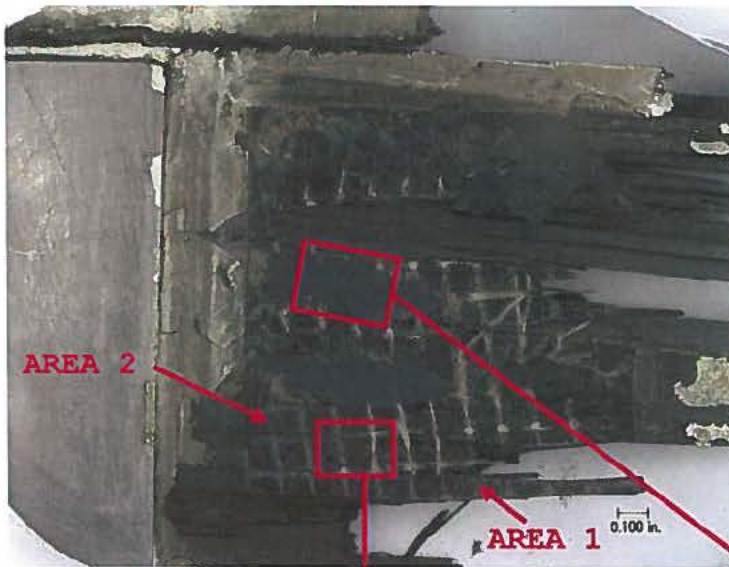


Figure 17

View of the red arm outboard side pivot retainer disbond. Close-up SEM views of Areas 1 and 2 are given in Figure 20.

Figure 18

Close-up view of area showing adhesive disbond of the primer from the retainer surface.



Figure 19

Close-up view of an area showing mixed adhesive and cohesive separation modes.

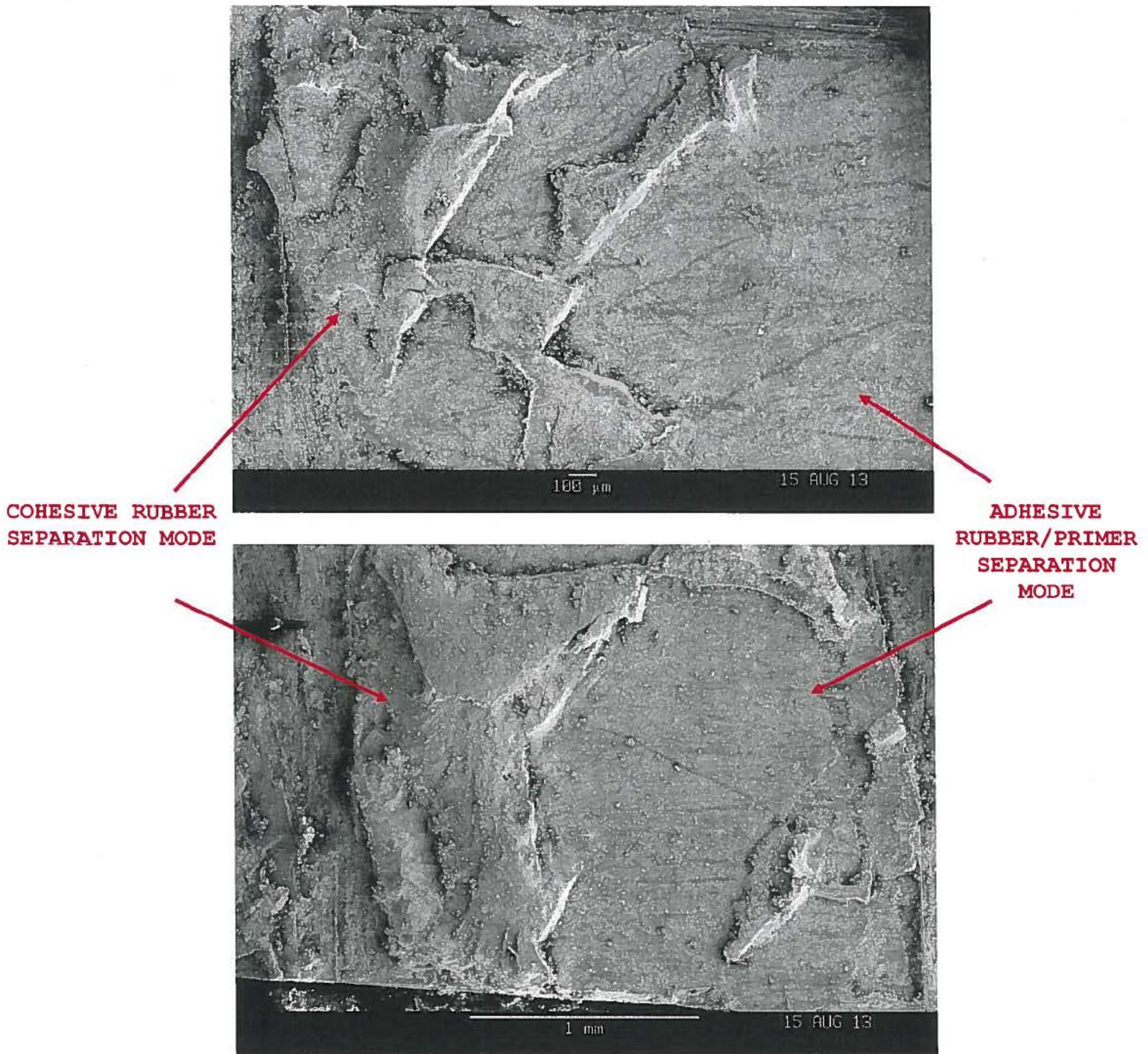


Figure 20

SEM view of Areas 1 (top) and 2 from Figure 17 showing adhesive and cohesive separation modes.

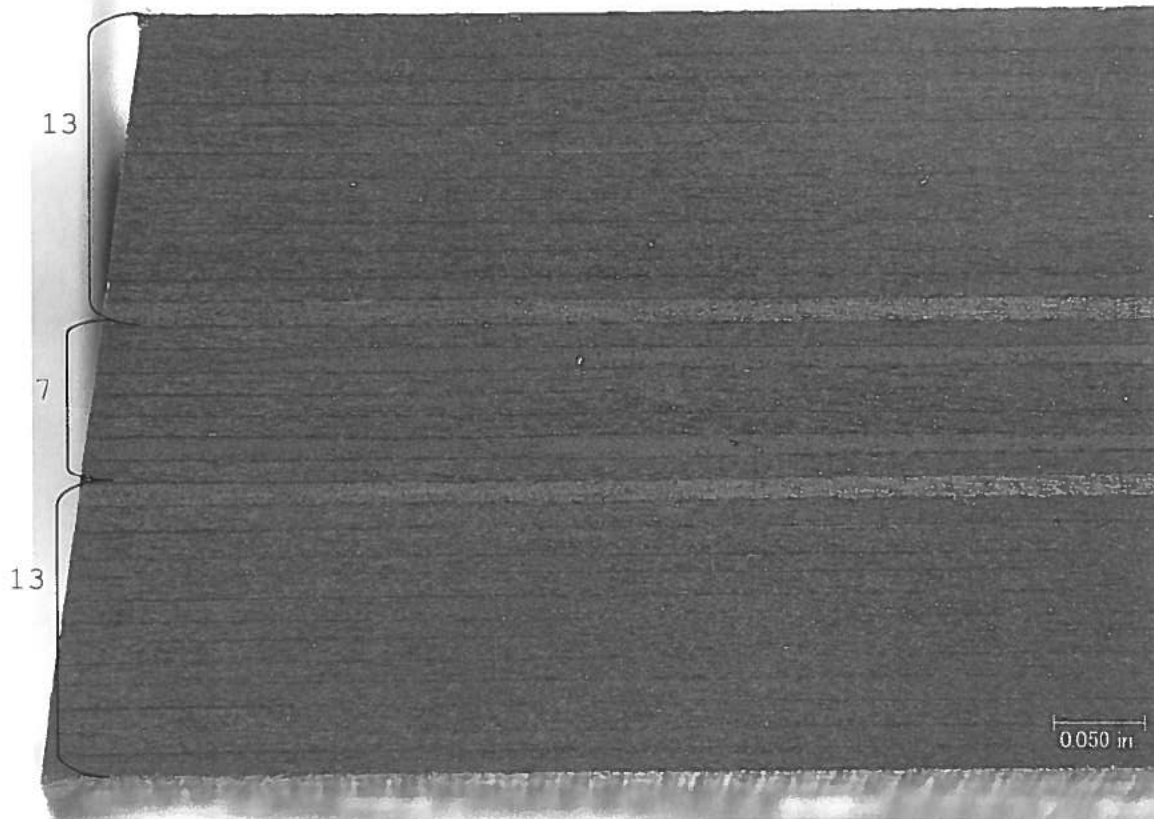


Figure 21

Trailing edge shown after polishing to reveal the ply lay-up. Lighter colored laminae represent the two  $+20^\circ$  plies identified on the drawing as plies 20 and 37. Thirty-three plies were present in all. No ply waviness was apparent.